



Riga Technical University Engineering High School

Development of Ta-TiO₂ nanoparticle-based transient optical memory material

Scientific research work in the field of materials science, engineering and technology group

Author:

Janis Stendzenieks
11th grade student

Supervisors:

Raivis Eglitis

Ph.D., RTU, Faculty of Natural Sciences and Technology Researcher

Jolanta Rimsa

Mg. Sc. Ing., RTU EHS chemistry teacher

Riga, 2024

Abstract

TiO₂ nanoparticles can be used in a very wide range of applications, and research on them can promote the development of various new technologies and concepts. Within the framework of the research, the concept of creating a transient optical memory material based on TiO₂ nanoparticles doped with tantalum is considered. The ability of these nanoparticles to react to ultraviolet light in the presence of an electron donor is examined. The optical properties of the nanoparticles are characterized by irradiating samples with UV light and determining the electrical resistance. Samples are prepared so that the electrical resistance can be measured for each individual pixel; the analyzed samples are made from both laboratory-made and commercially available electrodes. To test the proposed hypothesis, the prepared samples are evaluated for changes in electrical resistance over time and relative changes in electrical resistance. The data obtained in the study confirm the validity of the proposed hypothesis and the possibility of applying the discussed concept in the development of a new type of optical systems and the creation of transient optical memory materials.

The work is carried out at Riga Technical University, Faculty of Natural Sciences and Technologies from May 2023 to March 2024.

The paper is originally written in Latvian, contains 18 pages, 6 figures, 3 tables, 3 appendices, and uses 23 literature sources.

Keywords: TRANSIENT OPTICAL MEMORY, TANTALUM DOPED TiO₂, NANOPARTICLE OPTICAL ACTIVITY, ELECTRICAL RESISTANCE CHANGE, ULTRAVIOLET LIGHT.

Anotācija

TiO₂ nanodaļīņas iespējams izmantot ļoti plašā jomu spektrā, un pētījumi par tām spēj sekmēt dažādu jaunu tehnoloģiju un konceptu attīstību. Pētnieciskā darba ietvaros tiek aplūkots īslaicīgās optiskās atmiņas materiāla izveides koncepts, balstoties uz TiO₂ nanodaļīņu, kas dopētas ar tantālu, izmantošanu. Tieks apskatīta šo nanodaļīņu pārklājuma spēja reaģēt uz ultravioleto gaismu elektronu donora klātbūtnē. Nanodaļīņu optiskās īpašības tiek raksturotas, apstarojot paraugus ar UV gaismu un novērojot elektriskās pretestības izmaiņas. Paraugi ir sagatavoti tā, lai elektrisko pretestību varētu nomērīt katram individuālam pikselim; analizētie paraugi ir izstrādāti gan no laboratorijā veidoti, gan komerciāli izstrādātiem elektrodiem. Lai pārbaudītu izvirzīto hipotēzi, pagatavotajiem paraugiem nosaka elektriskās pretestības izmaiņu laikā, kā arī elektriskās pretestības relatīvo izmaiņu. Pētījumā iegūtie dati pierāda izvirzītās hipotēzes patiesumu un iespēju pielietot aplūkoto konceptu jauna tipa optisko sistēmu un īslaicīgās optiskās atmiņas materiālu izveidē.

Darbs izstrādāts RTU “Dabaszinātņu un tehnoloģiju fakultātē” no 2023. gada maija līdz 2024. gada martam.

Darbs rakstīts latviešu valodā, satur 16 lapas, 6 attēlus, 3 tabulas, 3 pielikumus un tajā izmantoti 23 literatūras avoti.

Atslēgas vārdi: ĪSLAICĪGĀ OPTISKĀ ATMIŅA, AR TANTĀLU DOPĒTS TiO₂, NANODAĻĪNU OPTISKĀ AKTIVITĀTE, ELEKTRISKĀS PRETESTĪBAS IZMAIŅA, ULTRAVIOLETĀ GAISMA.

Contents

| | |
|--|----|
| Introduction | 4 |
| 1. Literature overview | 5 |
| 1.1. Optically active materials..... | 5 |
| 1.1.1 Classification and properties of optically active materials..... | 5 |
| 1.1.2 Applications of optically active materials..... | 6 |
| 1.2. TiO ₂ nanoparticles | 6 |
| 1.2.1 Properties of TiO ₂ nanoparticles | 6 |
| 1.2.2 TiO ₂ nanoparticle synthesis..... | 7 |
| 1.2.3 Applications of TiO ₂ nanoparticles | 8 |
| 2. Experimental part..... | 9 |
| 2.1. ITO glass electrode samples..... | 9 |
| 2.2. Commercial electrode sample | 10 |
| 2.3. Measurements..... | 10 |
| 3. Results analysis | 11 |
| Conclusions | 16 |
| References | 17 |
| Appendices | 19 |

Introduction

The field of optically active materials is considered promising, as these materials can be used in various industries, such as the development of smoke detectors, medicine, and biotechnology [1]. One such material is titanium dioxide. In the field of optical materials, TiO_2 is often used in the form of nanoparticles, which exhibit suitable chemical and physical properties [2]. These nanoparticles are easily accessible and economically advantageous [2, 3]. They address challenges in cancer treatment, energy production, nanobiotechnology development, medicine, wastewater treatment, and many other diverse fields [2].

TiO_2 nanoparticles are used quite often as an optically active material [2]. The wide range of properties of TiO_2 nanoparticles, such as different crystalline structures, mechanical strength and optical activity under various types of radiation can ensure the development of optical technologies such as solar panels and gas sensors [1, 2]. In addition, the properties of nanoparticles and therefore their applications can be advanced using the so-called nanoparticle doping with other elements [4, 5]. Using these properties, new optical memory systems can be developed, potentially providing faster data transfer and lower power consumption for various electronic devices [6, 7].

For the development and investigation of such optical systems, the ability of TiO_2 nanoparticles to respond to ultraviolet light can be exploited [2]. This way, it is possible to create, for example, a 4-pixel system from several ITO (indium-tin oxide) electrodes, where changes in the electrical resistance of each pixel can be observed in the presence of ultraviolet radiation.

Hypothesis: When Ta-TiO₂ nanoparticle-coated ITO electrode pixels are irradiated with ultraviolet light, changes in the electrical resistance of the coating can be observed, specifically its reduction, as well as the reversibility of this effect.

Research objective: To develop different types of samples for which it is possible to measure the change in electrical resistance, as well as to examine how the electrical resistance of individual pixels is affected when they are shielded during ultraviolet light irradiation.

Tasks:

1. Create TiO_2 nanoparticle-coated samples with four pixels, for which the electrical resistance can be measured.
2. Measure the electrical resistance of the obtained samples in both ultraviolet light and standard radiation environments.
3. Test the reversibility of the resistance changes of these samples, as well as to observe the resistance change trends of individual shielded pixels.

1. Literature overview

To familiarize with the research topic and enhance understanding, the literature overview discusses the general classification of optical materials, the functions they perform, and their applications. Additionally, it provides information about the TiO₂ nanoparticles used within the scope of the research, including their properties, synthesis methods, applications, and other relevant parameters.

1.1. Optically active materials

Optically active materials represent a broad category encompassing a wide variety of materials with differing properties and applications in the development of new technologies. Today, they are associated with the operation of many technologies in the world, however, this field of science continues to develop rapidly. New discoveries about the properties, manufacturing methods, and potential future applications of these materials are constantly being made, alongside improvements and enhancements to existing optical material technologies. Below, the classification of optically active materials is examined, highlighting the characteristics and applications associated with each category.

1.1.1 Classification and properties of optically active materials

Optically active materials, based on their photonic structures and the ways in which the interaction between the material in question and light occurs, can be divided into 4 groups: thermal, chemical, electrical, and optical (light) [1].

Thermal mechanism materials, or phase change materials, exhibit notable optical properties based on their phase transitions between amorphous and crystalline states [8]. This type of optically active material offers many advantages, such as the ability to provide reversible optical processes, fast response mechanisms, and the fact that these materials are usually non-volatile [1, 8].

Optically active materials with chemical mechanisms rely on the occurrence of various chemical reactions [9]. Such reactions are, for example, the hydrogenation and dehydrogenation reactions of magnesium, in which magnesium is able to transition from its metallic, electrically conductive, state to magnesium dihydride, which is dielectric [1, 9]. This process results in an optically active material, although it is important to note that the hydrogenation and recovery processes are relatively slow [1].

Examples of optically active materials with electrical mechanisms include, for example, liquid crystals, which exist between a liquid and a crystalline state [10]. The light-refractive abilities of these crystals can be influenced not only by electrical, but also by chemical and thermal stimuli, which allows them to be used in a very wide range of photonic structures [1].

The operational mechanism of optically stimulated materials involves electrically conductive oxides and semiconductors, such as indium-tin oxide or indium-gallium-zinc oxide [1]. Based on the *Drude* model, the refractive index of semiconductors can be changed by configuring the charge densities of these semiconductors [1]. Consequently, the optical activity of these conductors and semiconductors is ensured by changing the free charge density, which in turn can be changed using various electrical or light optical impulses [1]. In this research work, the electrodes of the aforementioned indium-tin oxide semiconductor were used to develop the samples analyzed.

1.1.2 Applications of optically active materials

There exists a relatively wide range of optically active materials, each with specific properties, advantages, and limitations [1]. Below are some examples of possible uses for these materials:

1. smart dynamic screens - optically active materials can provide very high-resolution images with small-sized pixels using various electrochemical oxidation-reduction processes [11];
2. camouflage technology - materials with adaptive coloration properties, such as those utilizing electrochemical and thermal processes in gold and silver nanostructures or liquid crystals, can replicate camouflage processes observed in nature, such as those exhibited by certain octopus or chameleon species [1];
3. color filters - thanks to the effective light scattering of certain optically active materials, it is possible to create new, more advanced color filters that are able to provide much brighter colors, while also being much thinner than conventional color filters made with pigments [1, 12].
4. photonic memory devices - it is increasingly evident that electronic computer systems have reached their limits in terms of data processing capacity and speed. Due to this, a particularly important area of research for the development of future computer technologies is the study of photonic computer systems and the development and implementation of various basic computer components in the context of photonic devices, which are based on the properties of specific optical materials, which in turn could ensure the creation of new, fast and energy-efficient information storage and signal processing systems [6, 7].

1.2. TiO₂ nanoparticles

In recent years, the study of the properties, synthesis methods, and potential applications of TiO₂ nanoparticles has become a critical field of science, which can directly or indirectly contribute to advancements in many other disciplines [2]. The extensive applicability of TiO₂ nanoparticles is primarily due to their rich array of physical and chemical properties, as well as their availability.

Furthermore, several synthesis methods for producing various types of TiO₂ nanoparticles are known [2, 13]. The most significant properties of these nanoparticles, commonly used synthesis methods, and their applications in other scientific fields are further discussed. Additionally, the specific properties and synthesis methods of the TiO₂ nanoparticles used during the development of this study are briefly highlighted.

1.2.1 Properties of TiO₂ nanoparticles

Depending on their size and other parameters, TiO₂ nanoparticles possess a variety of chemical and physical properties. They can exhibit different crystalline structures, as well as unique optical and electrochemical properties [2].

Nanocrystalline TiO₂ predominantly exists in three different polymorphic forms: rutile, brookite, and anatase [2]. For instance, anatase crystalline type TiO₂ nanoparticles, due to their

high electron mobility, low dielectric constant and low density, are used in the production of solar panels [3]. During this research work, particles of the anatase crystalline type were used.

The ability of TiO₂ nanoparticles to transmit visible light ensures excellent optical properties [2]. Mechanical strength, chemical stability in solutions, phase composition, quality of the crystalline structure, particle size and other parameters can affect the optical activity of these nanoparticles [14].

The chemical and physical properties of TiO₂ nanoparticles are substantially affected by their electronic structure, particle size, surface characteristics, and arrangement [2, 13]. These parameters are considered critical determinants of crystal size [2].

The properties of TiO₂ nanoparticles can be enhanced through doping, which involves partial substitution of Ti in the nanoparticles [4, 5]. For example, doping TiO₂ with niobium, hafnium, or tantalum improves their photochromic properties [4, 5]. In this study, tantalum-doped TiO₂ nanoparticles are used.

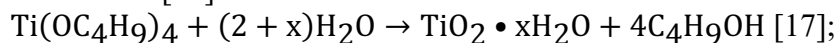
These nanoparticles have the ability to respond to UV (ultraviolet) light [2]. When they are irradiated with UV light, the valence electrons gain energy, thus being excited and forming electron deficiency regions, or electron holes [4]. These photoinduced electron holes can be filled using electron donors, such as butanol or ethanol [4]. As a result, a photoinduced electrical charge is generated within the particle environment, enabling changes in electrical resistance [4]. This makes TiO₂ nanoparticles applicable in photocatalysis and the development of various optical devices [2].

1.2.2 TiO₂ nanoparticle synthesis

TiO₂ nanoparticles can be synthesized using various methods, each with distinct advantages. Techniques such as hydrothermal synthesis, colloidal suspension, and vapor deposition are commonly used to produce nanotubes, nanofibers, nanoplates, and nanorods [2].

The hydrothermal method is usually carried out in steel pressure vessels at a specific temperature and pressure in the presence of NaOH [15]. The heating temperature may vary depending on the type of nanoparticles being produced. This method is suitable for producing TiO₂ nanotubes and nanoplates [2].

The colloidal suspension synthesis method can produce high purity homogeneous particles at relatively low temperatures [16]. TiO₂ nanoparticles are synthesized using titanium alkoxides, such as titanium butoxide (Ti(OC₄H₉)₄), through hydrolysis and condensation in a solvent like isopropanol. The general hydrolysis and condensation reaction in an aqueous medium can look like this [17]:



In the vapor deposition method, the material condenses or desublimates from the vapor phase to a liquid or solid [2]. There are two different vapor deposition synthesis methods – chemical, where a chemical reaction takes place in a vacuum vessel during the synthesis, and physical, where chemical reactions do not take place during the synthesis [18]. The condensation reaction is usually initiated by heating the gases in a vessel. By applying the principles of pyrolysis, it is possible to synthesize various types of TiO₂ nanoparticles in an oxygen or helium atmosphere [2].

The tantalum-doped TiO₂ nanoparticles used in this study were synthesized using titanium tetra n-butoxide, n-butanol, acetylacetone, tantalum (V) ethoxide, nitrogen gas, 4-dodecylbenzenesulfonic acid, deionized water, and methanol [4]. In this synthesis method, titanium tetra n-butoxide is added to a mixture of n-butanol and acetylacetone in a nitrogen gas environment, and a separate solution with tantalum ethoxide, n-butanol and acetylacetone is also formed [4]. The prepared solutions are then combined and a solution of 4-

dodecylbenzenesulfonic acid and deionized water are added [4]. The resulting solution is heated in several stages, then centrifuged and purified with methanol [4]. Finally, the formed tantalum doped TiO₂ nanoparticles are dispersed in n-butanol [4].

1.2.3 Applications of TiO₂ nanoparticles

TiO₂ nanoparticles are widely used in nanobiotechnology and nanomedicine research and technology development, for example, for the treatment of bacterial diseases, disinfecting microorganisms, cancer treatment, improvement of chemotherapy methods, development of coatings for orthopedic implants [2], as well as for improving *in vitro* and *in vivo* photodynamic cancer treatment therapies [19]. They can also be used in wastewater treatment, as photocatalysis degrades organic compounds in contaminated water [20]. In addition, by using TiO₂ nanoparticles for photocatalysis, it is also possible to improve air quality by reducing, for example, the concentration of nitrogen oxides [20].

TiO₂ nanoparticles are also used in energy production for the development of photovoltaic devices, such as nano-solar panels, smart windows and various sensors [16, 21]. These nanoparticles are also used to produce hydrogen from water splitting [22]. This method of producing hydrogen gas is advantageous because the hydrogen can be obtained in an environmentally friendly and cost-effective way, which is important due to the climate crisis and resource constraints [2].

Beyond these fields, TiO₂ nanoparticles are actively applied and studied in industries such as food, cosmetics, paper production, and pesticide degradation, among others [2].

2. Experimental part

As part of the research work, samples are developed in the form of a four-pixel system constructed from four electrodes. Real-time measurements of electrical resistance are performed for each pixel in both UV and standard lighting.

Through these measurements, data is obtained regarding changes in the electrical resistance of the embedded pixels over time, depending on the type of lighting they are exposed to. During the sample preparation process, all necessary safety precautions were followed, including the use of safety goggles and latex gloves. The reagents and sample components were sourced from "Acros" and "Ossila."

2.1. ITO glass electrode samples

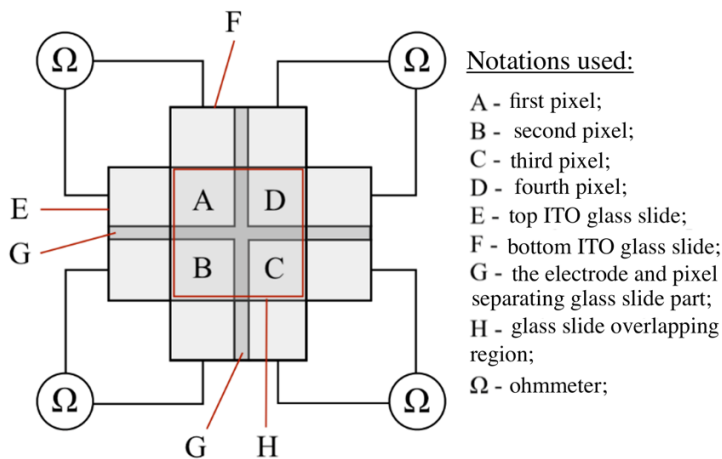


Figure 1. Schematic of the laboratory-made ITO electrode samples.

The electrodes forming the sample are constructed using two main components: ITO glass slides coated with a conductive layer and a colloidal solution of tantalum-doped TiO₂ nanoparticles (see Figure 1 and Appendix 1). In the following steps, three such laboratory-prepared electrode samples are created.

First, ITO slides are prepared - they are cut with a scalpel and a silicon carbide pencil, and the protective coating is removed in specific parts to separate individual pixels. Then they are etched for 15 minutes in 9M HCl. After that, the samples are washed with deionized water and placed in a plasma cleaner *Harrick Plasma PDC-002-CE*. The cleaned and degreased slides are then coated with the colloidal solution of tantalum-doped TiO₂ nanoparticles, using a micropipette and the *Laurell WS-650Mz-23NPPB* spin-coating device. The spin-coating device is set to a specific mode, where it first spins for 5 seconds at 500 rpm and then for another 30 seconds at 5000 rpm, with the micropipette volume set to 100 μl . After coating, the slides are dried in a laboratory oven at 150 °C for 60 minutes. After drying, the remaining protective film is removed and the formed slides are heat-treated at 400 °C for 2 hours. After heat treatment, the slides are cooled and arranged in pairs, where each pair of slides is intended to create one sample. A layer of ethanol is applied to one of the slides of the selected pair, and the other slide from the corresponding pair is placed on top of it. As a result, a sample is formed, where an ethanol layer is located between these two slides. To strengthen the created structure, epoxy glue is smeared along the sides of each sample. Then, thin copper wires are added to each of the obtained samples with silver paste.

2.2. Commercial electrode sample

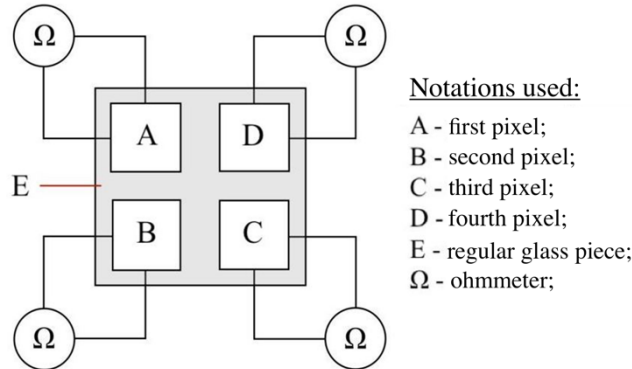


Figure 2. Schematic of a commercial electrode sample.

During the experiment, an additional sample was developed using industrially produced ITO electrodes (see Figure 2 and Appendix 2). Four *Micrux IDE-8 (10/10)* gold electrodes and the aforementioned colloidal solution of nanoparticles are used to create the four pixels.

First, the *Micrux* electrodes are taped with adhesive tape. The electrodes are cleaned in a plasma cleaner for 5 minutes, then the solution of Ta-TiO₂ nanoparticles is applied according to the previously described method, but with half the volume of solution used for each electrode. After applying the coating, the electrodes are dried in a drying oven at 150°C for 1 hour, then heat-treated at 400°C for 2 hours. After heating, the remaining parts of the tape are removed from the electrodes and a small piece of ordinary glass is cut off with a silicon carbide pencil. The 4 prepared *Micrux* electrode pixels are attached to the glass using double-sided adhesive tape, and two copper wires are attached to each of the electrodes with silver paste.

2.3. Measurements

The measurements are performed using the *Agilent 34970A* instrument, which is capable of measuring the electrical resistance of sample types in real-time. Y-shaped wires are screwed into the instrument cassette so that the branched ends of each wire are connected to compatible electrical cassette channels. To make it easier to determine which of the outgoing wires from the cassette corresponds to which cassette channel, and to navigate the connection of the wires to the corresponding sample electrodes, a label is attached to each of the wires, on which the corresponding *Agilent 34970A* cassette channel is written. The samples are attached to a laboratory stand and a UV lamp is attached at a fixed distance from the surface.

Once the resistance measuring device is installed and the sample to be analyzed is connected to the wires coming out of the device cassette, one of the sample pixels is covered with adhesive tape and the electrical resistance measurement is started. After obtaining the first resistance values under laboratory lighting, the UV light lamp is turned on. The sample is irradiated until it is possible to observe that the electrical resistance value has stabilized, meaning, the obtained real-time graph of electrical resistance versus time for each pixel no longer shows a decrease. Then the UV light lamp is turned off and the measurement is continued until the electrical resistance for each pixel stabilizes under laboratory lighting.

For the commercial electrode sample, the resistance measurements are carried out using similar procedures as before but there are a few nuances. Given the design of this sample, i.e., the fact that the electron donor substance ethanol is not integrated in this sample, during the measurement, the commercial sample is placed in a Petri dish, and ethanol is periodically dripped next to the sample. 50 microliters of ethanol are added every 7 minutes approximately.

3. Results analysis

The results of the electrical resistance measurements for all three laboratory-made ITO electrode samples (see Figures 3, 4 and 5) indicate a decrease in electrical resistance in each of the pixels embedded in the samples as a result of UV light irradiation. Since the resistance decreases not only quickly, but also very significantly, the values on the resistance axis in the created graphs are logarithmically transformed to base 10 for clarity. The value 10000 was chosen as the starting value of the logarithmic resistance axis. Additionally, for better visualization, the areas of the graph corresponding to the periods when the UV light lamp was turned on are shaded red.

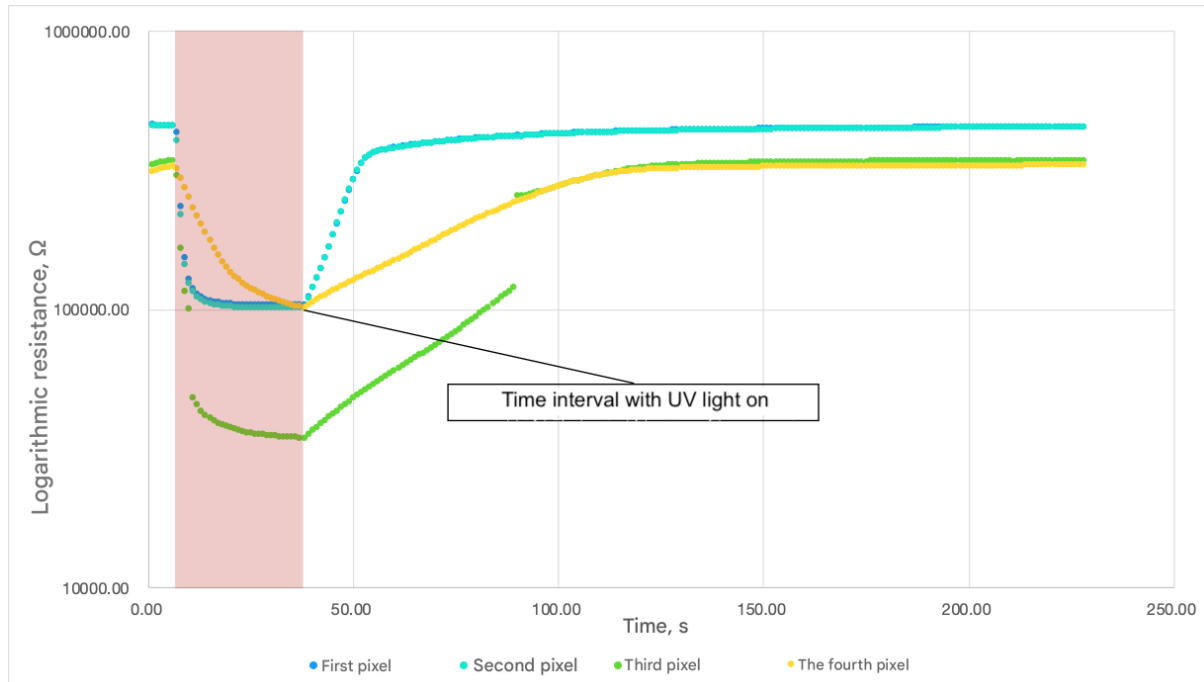


Figure 3. Logarithmic electrical resistance of pixels in the first sample as a function of time.

In the first sample, it can be observed that the electrical resistance of each pixel rapidly decreases after the UV light is turned on, which is followed by a stabilization period for the resistance values. A similar trend is observed in the other two samples (see Figures 4 and 5).

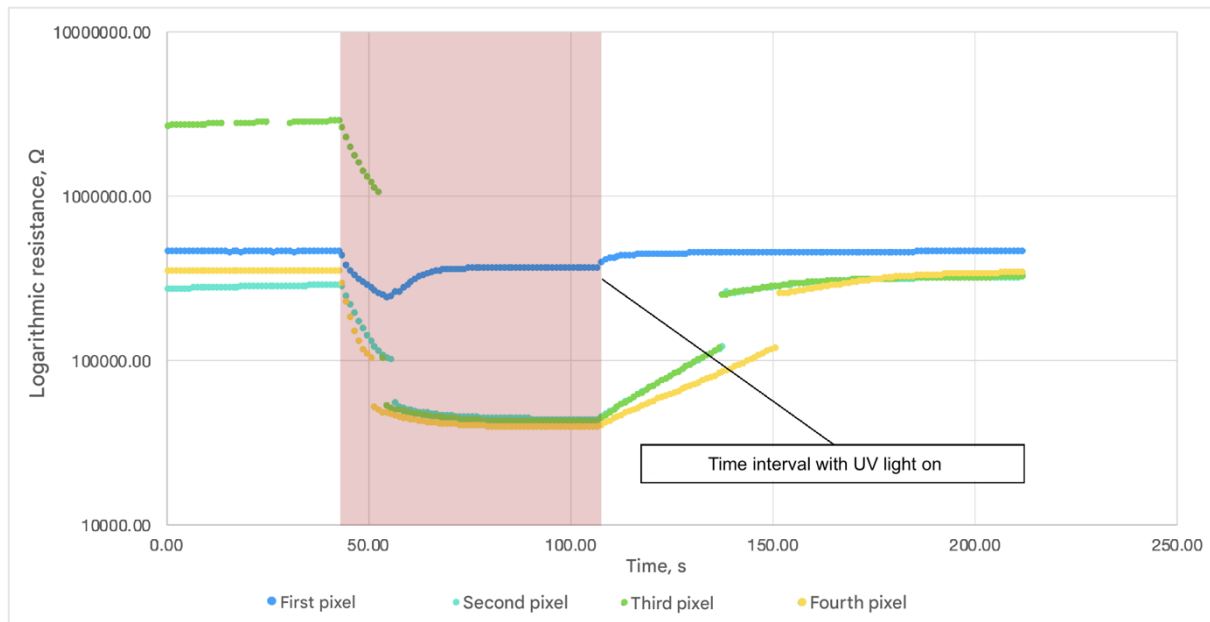


Figure 4. Logarithmic electrical resistance of pixels in the second sample as a function of time.

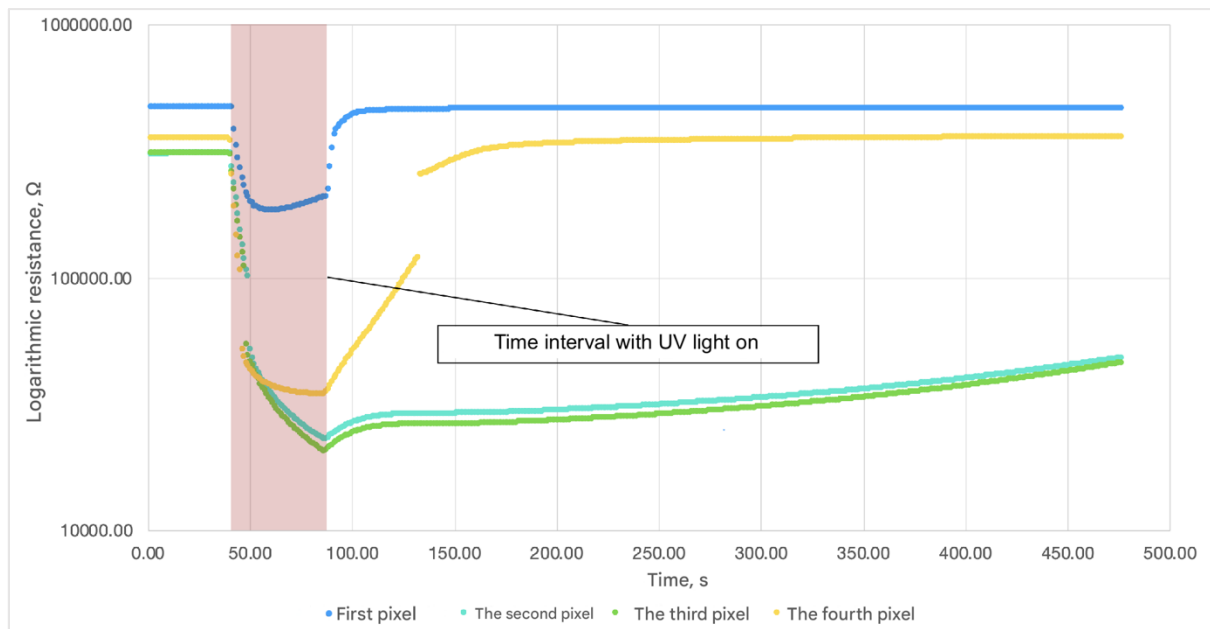


Figure 5. Logarithmic electrical resistance of pixels in the third sample as a function of time.

It should be noted that in all samples, the electrical resistances of the four pixels do not change equally under the influence of UV light; they are not identical even before the UV light is turned on. This can be explained by the nuances of the sample development methodology - it is very difficult to develop two samples that are identical in terms of resistance, since their resistance may depend on factors such as, for example, the unevenness of the nanoparticle coating used, which may occur during the coating application process.

In the first sample, the graph shows that after the exposure interval ends, the electrical resistance of each pixel gradually increases back to its initial value before UV exposure. However, a shift from this trend is observed for individual pixels of the second and third samples. For the third sample, it is possible to observe that the resistances of its first and fourth

pixels increase relatively quickly after turning off the UV light back to their initial value, while the resistances of the second and third pixels increase significantly more slowly and continue to grow even approximately 6 minutes after turning off the UV light. In the case of the second sample, it is possible to observe that the electrical resistance of the third pixel, unlike the other three pixels of the sample, does not increase to its initial resistance value after turning off the UV light. This can be attributed to possible irregularities in the electrical contact for the third pixel, as indicated by disruptions in the graph at the beginning of the measurement, representing resistance values too high for the *Agilent* 34970A device to measure accurately.

The irregularities of the electrical contact, as well as the self-calibration of the instrument itself during the measurement, are the reasons for the discontinuities in the resistance graphs, for example, for the fourth pixel of the third sample around the 50th and 140th second, for the fourth, third and second pixels of the second sample around the 50th and 150th second and for the third pixel of the first sample at the beginning of the measurement and around the 90th second. Despite this, the increase in resistance after turning off the UV light for the samples on average occurs slower than its decrease after turning on the UV light.

Additionally, the pixel resistance values within a single sample tend to be similar in pairs. For instance, in the first sample, the resistance curves of the first and second pixels, as well as those of the third and fourth pixels, align reasonably well. A similar phenomenon is also observed for the second and third pixels of the second sample, as well as the second and third pixels of the third sample. This can be explained by the specific design of the samples, namely their construction from two separate pieces of electrically conductive ITO glass, which also ensures this parity.

For each sample, the relative resistance change is calculated, where R_0 is the initial resistance before UV exposure, R is the resistance during exposure, and ΔR is the absolute difference between the two values. The relative resistance change was determined using the formula $\frac{R_0 - R}{R_0} = \frac{\Delta R}{R_0}$.

During the experiments, one pixel of each of these samples was covered with tape to observe whether the resistance change of these pixels under the influence of UV light irradiation would proceed differently than the others. The obtained values are summarized in Tables 1, 2 and 3.

Table 1. Relative resistance change in the first sample for each pixel.

| Pixel no. | Resistance before irradiation, Ω | Resistance during irradiation, Ω | Relative resistance change |
|-----------|---|---|----------------------------|
| First | 458428.02 | 102958.96 | 0.78 |
| Second | 457666.45 | 100836.06 | 0.78 |
| Third | 328177.45 | 34469.35 | 0.90 |
| Fourth | 312227.56 | 102745.38 | 0.67 |

Table 2. Relative resistance change in the second sample for each of the pixels.

| Pixel no. | Resistance before irradiation, Ω | Resistance during irradiation, Ω | Relative resistance change |
|-----------|---|---|----------------------------|
| First | 458289.94 | 364215.17 | 0.21 |
| Second | 268237.54 | 43471.16 | 0.84 |
| Third | 2663609.20 | 41995.82 | 0.98 |
| Fourth | 345577.12 | 38837.49 | 0.89 |

Table 3. Relative resistance change in the third sample for each of the pixels.

| Pixel no. | Resistance before irradiation, Ω | Resistance during irradiation, Ω | Relative resistance change |
|-----------|---|---|----------------------------|
| First | 466699.63 | 183062.19 | 0.61 |
| Second | 305686.24 | 34950.42 | 0.89 |
| Third | 306793.00 | 32499.35 | 0.89 |
| Fourth | 352778.61 | 37213.57 | 0.89 |

When one of the sample pixels is covered, its electrical resistance, in the case of perfect coverage, should ideally remain unchanged since the pixel is not exposed to UV light. However, since achieving perfect coverage and completely eliminating internal UV light reflection is challenging, it is expected that the electrical resistance of the covered pixels would not remain entirely unchanged but decrease to a lesser extent than the uncovered pixels. This effect should also be reflected in the relative resistance change values, namely, the masked pixels should have a smaller relative resistance change than the uncovered pixels. Analyzing Tables 1, 2 and 3, such a relationship can truly be observed. In the first sample, the data shows a significantly smaller relative resistance change for the fourth pixel, which was covered during the experiment (see Table 1). Similarly, in the second sample, the first pixel was covered, and its resistance change differs by more than a factor of four compared to the other pixels (see Table 2). A similar trend is also observed for the first pixel of the third sample, which was also covered with tape during the experiment. The relative electrical resistance change of this pixel is approximately 0.28 smaller than the values obtained for the other pixels (see Table 3).

The commercial electrode sample was analyzed using methods similar to those used for the laboratory-produced electrode samples. For the commercial electrode sample, a sharp decrease in electrical resistance after the UV light was switched on can also be clearly observed (see Figure 6). After the end of the irradiation interval, the electrical resistance of the first, second and fourth pixels of the sample begins to gradually increase to the initial value before UV irradiation.

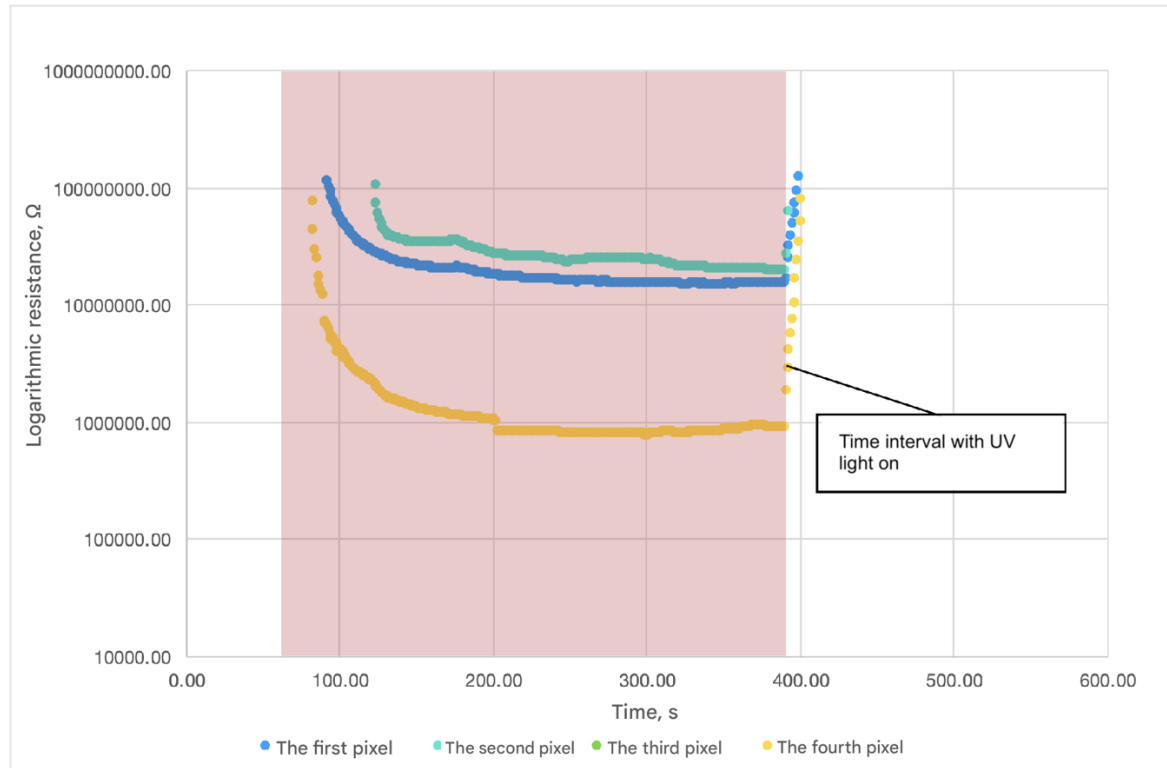


Figure 6. Logarithmic electrical resistance of pixels in the commercial electrode sample as a function of time.

The decrease in electrical resistance can be observed for the first, second and fourth pixels, however, it can be seen in the graph that several data points are missing for both the first, second and fourth pixels at the beginning and end of the measurement. In these areas, when performing resistance measurements, the electrical resistance of the pixels is so high that the equipment used for the measurements is unable to register them. Consequently, the first data points appear only briefly after the UV light is turned on, when the resistance has decreased to a value that the equipment can read. The data curves are interrupted shortly after the UV light is turned off, when the electrical resistance again reaches a value so high that the *Agilent* device cannot read it.

A similar data gap can be observed for the third pixel throughout the entire measurement. This phenomenon is linked to the fact that, in the case of the commercial electrode sample, one of the pixels was also covered with tape to examine the electrical resistance change tendencies of a covered pixel under the influence of UV light. Unlike the laboratory-produced ITO electrode samples, the commercial sample does not exhibit the phenomenon of internal reflection between pixels when the pixel is correctly covered. This is because each pixel is individually separated and attached to a laboratory glass piece with double-sided tape. For this reason, at no time did the electrical resistance of this pixel under the influence of UV light drop to such a level that the measuring device could register any resistance value. Consequently, it is also not possible to fully determine the relative resistance change of each pixel for this sample, since the highest possible resistance values are not registered. Despite this, it can be concluded that pixel 3 is obscured, since internal reflection does not occur in the commercial electrode sample.

Conclusions

1. The proposed hypothesis is confirmed: when irradiating ITO electrode pixels coated with Ta-TiO₂ nanoparticles with ultraviolet light, changes in electrical resistance, specifically a decrease, can be observed in the coating, as well as the reversibility of this effect.
2. Using the methodology applied in the research work, it is possible to create a 4-pixel system from several ITO conductive glass pieces or commercially developed electrodes, in which the change in the electrical resistance of each pixel in the presence of ultraviolet radiation can be observed.
3. Both laboratory-made ITO electrode samples and commercial *Micrux* IDE-8 electrode samples demonstrate a rapid decrease in electrical resistance as a result of ultraviolet light irradiation. Within a short time interval, the relative resistance change of pixels not covered with tape can reach up to 0.98.
4. The reversibility of resistance changes is well evident in the created samples, that is, after the irradiation with ultraviolet light is stopped, the electrical resistance of the samples begins to increase back to its original value.
5. Using the methodology outlined in this work, it is possible to validate the concept of creating a short-term optical memory material based on optical impulse charge induction. However, it is challenging to ensure identical base electrical resistance within the pixels of the samples.
6. For the laboratory-made ITO electrode samples, the pixels covered during irradiation also exhibit a decrease in electrical resistance due to internal reflection of UV light within the ITO glass. However, this decrease occurs more slowly than in uncovered pixels.
7. The covered pixel in the commercial electrode sample is significantly less affected by the factor of internal reflection of ultraviolet light due to the sample's design, which ensures the separation of individual pixels.

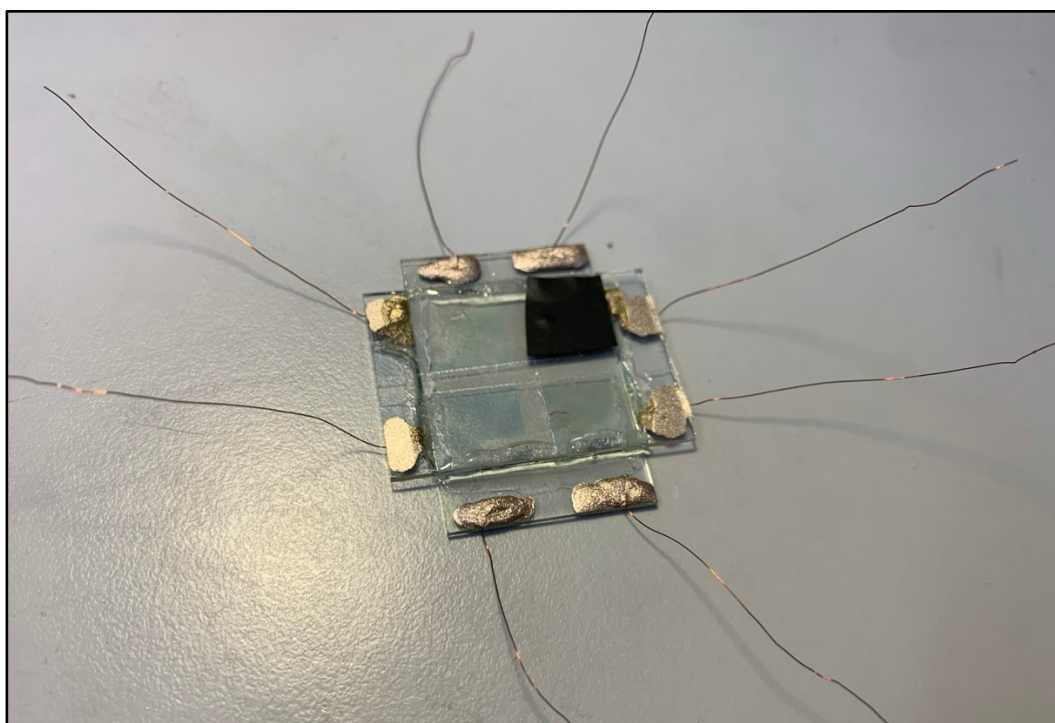
References

1. Ko, JH, Yoo , YJ, Lee , Y., Jeong , H.-H., Song , YM: A review of tunable photonics : Optically active material and applications from visible to terahertz . (2022). <https://doi.org/10.1016/j.isci>
2. Akakuru , OU, Iqbal , ZM, Wu , A.: 2 Nanoparticles , 6 Applications of TiO 2 Nanoparticles , 14 Conclusion . (2020)
3. Gupta , SM, Tripathi , M.: A review of TiO2 nanoparticles . Chinese Science Bulletin . 56, 1639–1657 (2011). <https://doi.org/10.1007/s11434-011-4476-1>
4. Eglītis, R., Kraukle, A., Käämbre , T., Šmits, K., Ignatāns , R., Rubenis, K., Šutka , A.: Nb , Ta and Hf – The tri-dopant tournament for the enhancement of TiO2 photochromism . J Photochem Photobiol A Chem. 439, (2023). <https://doi.org/10.1016/j.jphotochem.2023.114620>
5. Almutairi , B., Ali, D., Alyami , N., Alothman , NS, Alakhtani , S., Alarifi , S.: Tantalum doped TiO2 nanoparticles induced cytotoxicity and DNA damage through ROS generation in human neuroblastoma cells . J King Saud University Sci . 33, 101546 (2021). <https://doi.org/10.1016/j.jksus.2021.101546>
6. Chen , X., Xue , Y., Sun , Y., Shen , J., Song , S., Zhu , M., Song , Z., Cheng , Z., Zhou , P.: Neuromorphic Photonics Memory Devices Using Ultrafast , Non- Volatile Phase Change Materials . Advanced Materials . 35, (2023). <https://doi.org/10.1002/adma.202203909>
7. Cheng , Z., Ríos , C., Youngblood , N., Wright , CD, Pernice , WHP, Bhaskaran , H.: Device-Level Photonics Memories and Logic Applications Using Phase Change Materials . Advanced Materials . 30, (2018). <https://doi.org/10.1002/adma.201802435>
8. Hempelmann , J., Müller , PC, Ertural , C., Dronskowski , R.: The Orbital Origins of Chemical Bonding in Ge – Sb –Te Phase-Change Materials **. Applied Chemistry International Edition . 61, (2022). <https://doi.org/10.1002/anie.202115778>
9. Duan , X., Kamin , S., Sterl , F., Giessen , H., Liu, N.: Hydrogen-Regulated Chiral Nanoplasmonics . Nano Lett . 16, 1462–1466 (2016). <https://doi.org/10.1021/acs.nanolett.5b05105>
10. Stevenson , CL, Bennett , DB, Lechuga-Ballesteros , D.: Pharmaceutical Liquid Crystals : The Relevance of Partially Ordered Systems . J Pharm Sci . 94, 1861–1880 (2005). <https://doi.org/10.1002/jps.20435>
11. Hosseini , P., Wright , CD, Bhaskaran , H.: An optoelectronic framework enabled by low-dimensional phase change film . Nature. 511, 206–211 (2014). <https://doi.org/10.1038/nature13487>
12. He , Q., Youngblood , N., Cheng , Z., Miao , X., Bhaskaran , H.: Dynamically tunable transmissive color filters using ultra-thin phase change material . Opt Express. 28, 39841 (2020). <https://doi.org/10.1364/OE.411874>
13. Bai , Y., Mora- Seró , I., De Angelis , F., Bisquert , J., Wang , P.: Titanium Dioxide Nanomaterial for Photovoltaic Applications . Chem Rev. 114, 10095–10130 (2014). <https://doi.org/10.1021/cr400606n>
14. Govindasamy , G., Murugasen , P., Sagadevan , S.: Investigations there the Synthesis , Optical and Electrical Properties of TiO2 Thin Movie by Chemical Bath Deposition (CBD) method . Materials Research . 19, 413–419 (2016). <https://doi.org/10.1590/1980-5373-MR-2015-0411>

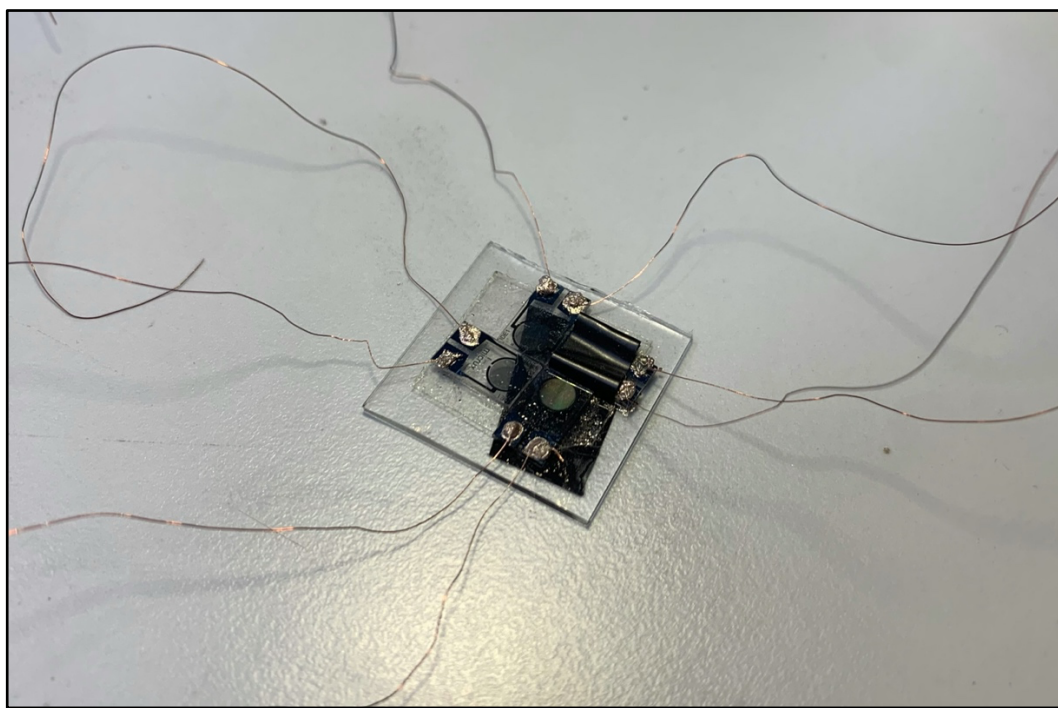
15. Dawson , G., Chen , W., Zhang , T., Chen , Z., Cheng , X.: A study there the effect of starting material phase there the production of trititanium nanotubes . Solid State Sci . 12, 2170–2176 (2010). <https://doi.org/10.1016/j.solidstatesciences.2010.09.019>
16. Sa'adah , U., Himmah , SW, Suprayogi , T., Diantoro , M.: ScienceDirect Peer review under responsibility of the scientific The Effect of Time Deposition of PAN / TiO₂ Electrospun there Photocurrent Performance of Dye-Sensitized Solar Cell . (2018)
17. Lee , HY, Kale, GM: Hydrothermal Synthesis and Characterization of Nano-TiO₂. Int J Appl Ceram Technol . 5, 657–665 (2008). <https://doi.org/10.1111/j.1744-7402.2008.02248.x>
18. Ayllón , JA, Figueras , A., Garelík , S., Spirkova , L., Durand , J., Cot , L.: Preparation of TiO₂ powder using titanium tetraisopropoxide decomposition in a plasma enhanced chemical steam deposition (PECVD) reactor . J Mater Science Lett . 18, 1319–1321 (1999). <https://doi.org/10.1023/A:1006657510154>
19. Bosetti , M., Massè , A., Tobin, E., Cannas , M.: Silver coated material for external fixation devices : in in vitro biocompatibility and genotoxicity . Biomaterial . 23, 887–892 (2002). [https://doi.org/10.1016/S0142-9612\(01\)00198-3](https://doi.org/10.1016/S0142-9612(01)00198-3)
20. Fujishima , A., Honda, K.: Electrochemical photolysis of water at a semiconductor electrode . Nature. 238, 37–38 (1972). <https://doi.org/10.1038/238037a0>
21. Bai , Y., Mora- Seró , I., De Angelis , F., Bisquert , J., Wang , P.: Titanium dioxide nanomaterial for photovoltaic applications . Chem Rev. 114, 10095–130 (2014). <https://doi.org/10.1021/cr400606n>
22. Maeda , K., Xiong , A., Yoshinaga , T., Ikeda , T., Sakamoto , N., Hisatomi , T., Takashima , M., Lu , D., Kanehara , M., Setoyama , T. , Teranishi , T., Domen , K.: Photocatalytic overalls water splitting promoted by two different cocatalysts for hydrogen and oxygen evolution under visible light . Angew Chem Int Ed Engl. 49, 4096–9 (2010). <https://doi.org/10.1002/anie.201001259>

Appendices

Appendix 1. Laboratory-made ITO electrode sample.



Appendix 2. Commercial Micrux electrode sample.



Appendix 3. National student scientific research conference poster in Latvian.

Uz Ta-TiO₂ nanodaļīnām balstīta īslaicīgās optiskās atmiņas materiāla izveide

Zinātniskās pētniecības darbs inženierzinātnes un tehnoloģijas nozaru grupas materiālzinātnes nozarē



Darba autors: Jānis Stendzenieks, RTU inženierzinātņu vidusskolas 11. klases skolēns

Darba vadītāji: Mg. sc. Ing. Jolanta Rimša, RTU inženierzinātņu vidusskolas ķīmijas skolotāja, Ph.D. Raivis Egličis, RTU Dabaszinātņu un tehnoloģiju fakultātes pētnieks

AKTUALITĀTE

- Alternatīvas informācijas glabāšanas sistēmas izveide, kas spētu patēri Mazāk energijas, tādējādi nodrošinot arī ātrāku datu pārnesi un uzlabojot dažādu intensīvu uzdevumu veikspēju.
- Kvantu datoru un optisko impulsu elektronikas pirmatnējo komponēnu izstrāde un attīstība.

DARBA MĒRKIS UN HIPOTĒZE

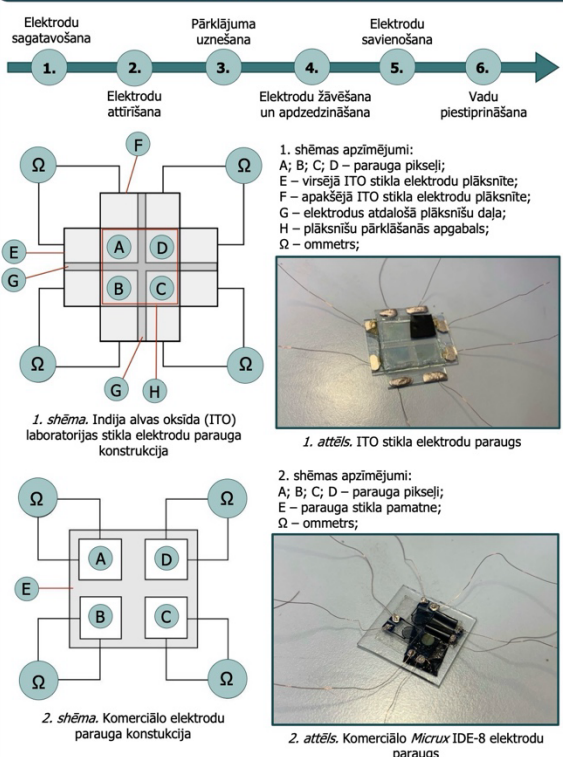
Darba mērķis: Izstrādāt dažādu tipu paraugus, kurus apstarojo ar ultravioleto (UV) gaismu iespējams novērot elektriskās pretestības izmaiņas, kā arī pārbaudit paraugu atsevišķu pikselu elektriskā pretestību izmaiņas tendences.

Hipotēze: Ar ultravioleto gaismu apstarojo ar Ta-TiO₂ nanodaļīnām pārkārtīgi ITO elektrodu pikselus, iespējams novērot izmaiņas pikselu elektriskajā pretestībā, proti, tās samazināšanos, kā arī novērot šo efektu atgriezeniskumu.

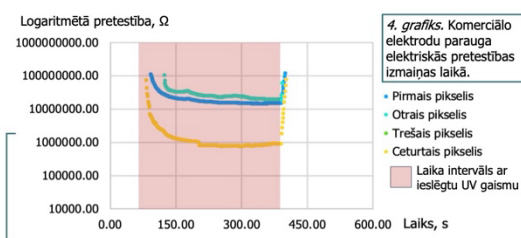
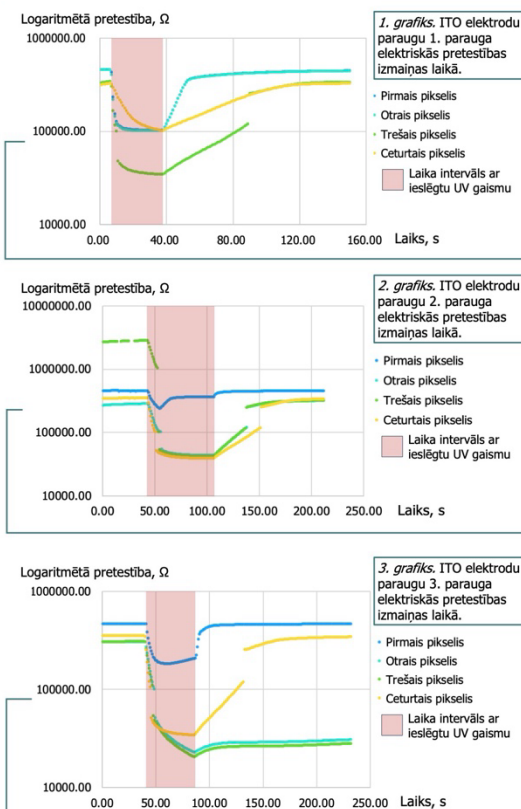
DARBA UZDEVUMI

- Izveidot ar TiO₂ nanodaļīnām pārkārtīgi paraugus ar četriem pikseliem, kuriem iespējams nomērīt elektriskā pretestību.
- Nomērīt iegūto paraugu elektriskā pretestību gan UV apgaismojumā, gan standarta apgaismojuma vidē.
- Pārbaudit šo paraugu pretestības izmaiņu atgriezeniskumu, kā arī novērot atsevišķu aizklāto pikselu pretestības izmaiņas tendences.

PARAUGU IZSTRĀDE



REZULTĀTI



SECINĀJUMI

- Izvirzīta hipotēze apstiprinās, proti, ar ultravioleto gaismu apstarojo ar Ta-TiO₂ nanodaļīnām pārkārtīgi ITO elektrodu pikselus, iespējams novērot elektriskās pretestības samazināšanos, kā arī šo efektu atgriezeniskumu.
- Izmantojot pētniecisku darba ietvaros pielietoto metodiķu, var tikt izvēldots optiskās aktīvās materiāls no vairākiem ITO elektrovdalītējiem stikliem vai komerciāli izstrādātiem elektrodiem, kurā var novērot atsevišķu pikselu elektriskās pretestības izmaiņas ultravioletā starojuma ietekmē.
- Gan laboratorijā veidoto ITO elektrodu, gan komerciāli izmantoto Micru IDE-8 elektrodo paraugiem elektriskās pretestības samazināšanās ultravioletā starojuma ietekmē norisinās strauji. Šāda laika intervāla to pretestības relatīvā izmaiņa ar lēmīti neaizklātajiem pikseliem spēj sasniegt līdz 0,98.
- Laboratorijā veidoto ITO elektrodo paraugus iestrādātajiem pikseliem, kuri apstarošanas laikā ir aizklāti, arī tiek novērots elektriskās pretestības samazināšanās gaismas iekšējais astarošanās dēļ, tomēr tā norit lēnāk, nekā neaizklātajiem pikseliem. Šāds fenomens nav novērjams komerciālo elektrodo parauga gadījumā.